J. Fluid Mech. (1990), *vol.* 214, *pp.* 503–515
Printed in Great Britain

Viscous sintering: the surface-tension-driven flow of a liquid form under the influence of curvature gradients at its surface

By H. K. KUIKEN
Philips Research Laboratories, P.O. Box 80.000, 5600 JA Eindhoven, The Netherlands

(Received 23 September 1988 and in revised form 20 October 1989)

A boundary-element method is applied to solve the equations describing the deformation of a two-dimensional liquid region under the influence of gradients of the curvature of its outer boundary. This research is motivated by a desire to obtain a better understanding of viscous sintering processes in which a granular compact is heated to a temperature at which the viscosity of the constituent material becomes low enough for surface tension to cause adjacent particles to deform and coalesce. The boundary-element method is capable of showing how a moderately curved initial shape transforms itself into a circle. Initial shapes showing more extreme curvature gradients, which are relevant in the initial stages of a sintering process, cannot be dealt with by the boundary-element method in its present form. The numerical solution of the continuous model shows a tendency to create oscillations in the outer boundary of the liquid region. On the other hand, an analytical small-amplitude analysis shows that rapid oscillations vanish exponentially fast.

1. Introduction

Sintering is a technique in which a compact consisting of many particles is heated to a temperature at which the mobility of the material is so high that contiguous particles coalesce. As a result, the cohesion of the compact increases with time. One of the oldest applications of this technology is to be found in the brick industry. However, nature itself shows many examples of sintering phenomena which predate human application of this technology by millions of years. The formation of rock strata from sandy sediments under the influence of high pressures exerted by later depositions is one such example.

The whole complex of sintering phenomena cannot be explained on the basis of a single physical principle. Along with the great variety of materials in the physical world, a number of physical principles can be responsible for sintering in each particular case. Referring to a recent review by Exner (1979), we may mention (i) volume diffusion or (ii) surface diffusion of vacancies in the atomic structures of the materials involved, (iii) evaporation followed by condensation, and (iv) volume flow (viscous, plastic, viscoelastic, etc.) driven by surface tension. The last of these will concern us here.

A relatively recent application of sintering is the production of high-quality glasses by means of what is known as the sol-gel technique. In this technique a gel consisting of a maze of interconnecting glassy strands and particles is grown from a suspension. A popular description of such an aerogel, which is extremely light as most of its volume is taken up by air, has recently been given by Fricke (1988). When the

aerogel is heated to sufficiently high temperatures, the viscosity of the glass becomes low enough for surface tension acting on the interior surface of the gel to cause the gel to collapse into a dense homogeneous material. Ideally, the final product is free of voids, and a high-quality glass is obtained that can be used, for instance, in the production of glass fibres for the telecommunications industry.

Clearly, a deterministic description of the viscous flow of a structure as complicated as an aerogel is out of the question, even when we restrict ourselves to a simple Newtonian constitutive model. The structure is simply too stochastic for such an attempt to be successful. Recently, Scherer (1977, 1984) described another approach in which the gel is modelled by a regular three-dimensional array of interconnected liquid cylinders. On the basis of this model he was able to define a unit cell within this structure, and calculate its surface. Next, Scherer applied a rule, first introduced in the context of sintering by Frenkel (1945), namely that the work done by surface tension in decreasing the interior surface must be equal to the total heat produced by dissipation. It is here that a practical difficulty arises. To be able to calculate the dissipated heat, one must first give an exact description of the flow field. Scherer remarks quite rightly that it would be unrealistic to give an exact description of the fluid flow in a structure as complex as his unit cell, which, in itself, only roughly approximates to reality. He therefore proposes an approximate description of the flow, and likewise obtains a rough estimate of the heat produced. His main result is a graph showing the density of the gel as a function of time.

Scherer's analysis breaks down when the gel can no longer be modelled as an array of interconnecting liquid cylindrical bridges. This happens in the later stages of the process, when adjacent glass surfaces touch and pores are formed. In the earlier days of sintering theory Mackenzie & Shuttleworth (1949) made an attempt at describing the dynamics of a compact with pores distributed throughout. Their approach was to distinguish the immediate neighbourhood of an individual pore and its farther surroundings. In the latter region the interplay between pores and liquid was summed, and this behaviour was somehow matched to the flow in the immediate vicinity of the particular pore under observation. These authors also applied Frenkel's principle, coming up with a law describing the density of the compact as a function of time.

Although, as we have already concluded, a deterministic description of the microscopic flow within an actual sintering compact is out of the question, much as it would be unrealistic to describe the mechanical behaviour of a macroscopic body on the basis of our knowledge of interatomic forces, scientists studying sintering phenomena have long been interested in the behaviour of very simple systems, for instance the coalescing of two spheres, or the sintering of a sphere onto a flat surface. In terms of our earlier simile we could call this the 'atomic' theory of sintering. Although it is doubtful whether the fruits of this type of research will tell us directly how to deal with far more complex macroscopic systems, we may be able to extract constitutive laws from them. The correct constitutive laws will eventually enable us to develop a phenomenological theory for macroscopic systems.

One of the first to study simple systems in a more or less systematic manner was Kuczinsky (1949*a*, *b*). He performed a number of experiments and applied Frenkel's theory to derive an analytical description of his results. He was particularly interested in the diameter of the neck region between the two spheres as a function of the time. If this diameter is denoted by d and the time by t, then Frenkel's principle tells us that $d \propto t^{\frac{1}{2}}$. If the driving force behind the sintering process is not surface tension, but rather one of the other physical principles we mentioned earlier,

then theories as simple as those of Frenkel's lead to other exponents in the d *vs.* t relationship. This has placed a diagnostic tool in the hands of sintering scientists. Later the study of simple systems remained an integral part of sintering science, and we refer to authoritative reviews by Geguzin (1973) and Exner (1979) for more information.

In this paper we shall present a method by which one can obtain an exact description of the sintering of simple systems, i.e. rather than using a global rule such as Frenkel's, which only uses a rough estimate of the influence of viscous effects, we shall define the problem in terms of the field equations appertaining to viscous flow. Our aim is to develop a method which tells us how an arbitrarily shaped blob, driven by surface tension acting at its own outer boundary, transforms itself through time, ending as a perfectly round form. In order to limit the technical difficulties somewhat, we shall study only two-dimensional shapes here. As we shall see, it is the gradient of the curvature of the outer boundary which is the driving force. Obviously, this force is equal to zero for a circle.

The numerical technique that we shall use to solve the model is one employing boundary elements. The problem is formulated first as a set of partial differential equations with boundary conditions. The partial differential equations are solved formally, which results in a set of integral equations involving the, as yet unknown, values of the dependent variables and their normal derivatives on the boundary. In many respects we shall follow the approach of Ingham & Kelmanson (1984) who applied the method to a number of potential and biharmonic problems, and, in doing so, demonstrated its effectiveness in solving them. This approach is numerical in that the boundary is replaced by a polygon. The integrals appearing in the integral equations are replaced by sums of integrals, one along each of the sides of the polygon. However, whereas Ingham & Kelmanson approximate the dependent variables by constant values on each of the sides of the polygon, we shall strive for greater accuracy by taking continuous approximations for these unknowns, which vary linearly along each of the subregions of the polygon. Also, whereas these authors try to fit their unknown boundary within a framework that involves a given function with a few free parameters, we shall track the boundary on the basis of the velocity field obtained after solving the equations.

2. Equations and boundary conditions

We consider a two-dimensional incompressible fluid flow that is characterized by the physical parameters η, the dynamic viscosity; γ, the surface tension; and l, which is a characteristic length. The dimensions of these parameters are N s m^{-2}, N m^{-1} and m respectively. On the basis of these three parameters we can define a characteristic velocity u_c, a characteristic pressure p_c and a characteristic time t_c as follows:

$$u_c = \frac{\gamma}{\eta}, \quad p_c = \frac{\gamma}{l}, \quad t_c = \frac{l\eta}{\gamma}. \tag{1}$$

Henceforth, we shall assume that all variables, both the dependent and the independent ones, have been rendered dimensionless by means of u_c, p_c, t_c and l, or combinations of these values.

If the Reynolds number

$$Re = \frac{u_c l\rho}{\eta} = \frac{\gamma l\rho}{\eta^2}, \tag{2}$$

where ρ is the density (kg m^{-3}) of the fluid, is much less than unity, the creeping-flow

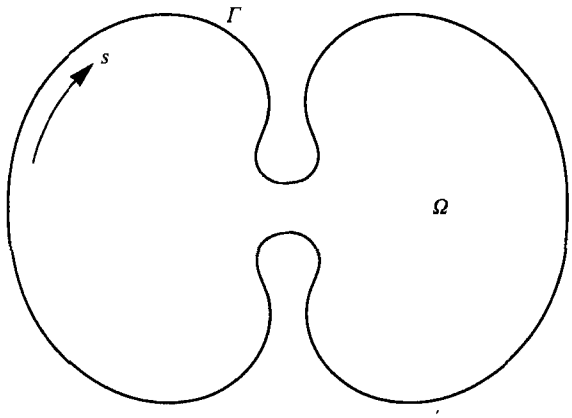

FIGURE 1. Geometrical configuration.

equations are valid. For a typical sintering system consisting of a glassy aerogel we have (Reed 1988, p. 462) $\eta \approx 10^8$ N s m^{-2} and $\gamma \approx 10^{-1}$ N m^{-1}. The particle size can be put at a few microns, although initially it can be much smaller. Therefore, u_c is of the order of 10^{-9} m s^{-1} which means that the process is extremely slow. For this system Re is of the order of 10^{-19}.

Our region of flow is defined by a closed curve Γ which encloses an area denoted by Ω (figure 1). In terms of the stream function ψ and the vorticity ω the governing equations, which are valid in $\Omega+\Gamma$, are (Batchelor 1967)

$$\nabla^2\psi = \omega, \tag{3}$$

$$\nabla^2\omega = 0. \tag{4}$$

Since Γ is a moving boundary, we need three boundary conditions. Two of these can be derived in the manner explained by Ingham & Kelmanson (1984, chap. 5). Requiring that the component of the stress vector along Γ is equal to zero, we have

$$\omega = 2\frac{\partial^2\psi}{\partial s^2} - 2\kappa(s)\psi' \quad \text{on} \quad \Gamma, \tag{5}$$

where we have written ψ' instead of $\partial\psi/\partial n$. The normal component of the stress vector is proportional to the local curvature of Γ. This condition is expressed as follows:

$$2\frac{\partial^2\psi'}{\partial s^2} + 2\frac{\partial}{\partial s}\kappa\frac{\partial\psi}{\partial s} + \omega' = -\frac{\mathrm{d}\kappa}{\mathrm{d}s} \quad \text{on} \quad \Gamma, \tag{6}$$

where s is the arclength along Γ and κ is the curvature function. The details of the derivation of the equations can be found in a companion paper (Kuiken 1990).

Assuming, for the sake of argument, that Γ is fixed, we must conclude that the solution to the problem defined by (3)–(6) will lead, in general, to a non-zero flow field on Γ. This would mean an inflow through one part of Γ and an outflow elsewhere. Since Γ is a material boundary, this cannot be accepted. Therefore, the displacement of Γ follows from the velocity field just defined. This leads to our third boundary condition:

$$\frac{\mathrm{d}x}{\mathrm{d}\tau} = \frac{\partial\psi}{\partial y}\bigg|_\Gamma, \quad \frac{\mathrm{d}y}{\mathrm{d}\tau} = -\frac{\partial\psi}{\partial x}\bigg|_\Gamma, \tag{7}$$

where τ is the dimensionless time,

subject to the initial conditions

$$x = x_A, \quad y = y_A \quad \text{at} \quad \tau = \tau_0. \tag{8}$$

It is interesting to note that for given Γ, the equations and boundary conditions (3)–(6) are linear and homogeneous, except for the non-homogeneous right-hand side of (6). Thus, the forcing term in this problem is the derivative of the curvature κ along the curve Γ. When κ is constant all along Γ, i.e. when Γ is a circle, the forcing term is zero. Apparently, this is the state the system will seek to attain, which will be achieved after successive applications of (7) and (8).

3. Solution method

A formal solution to (3) and (4) can be given in terms of the values of the unknowns on the boundary Γ. Evaluating this solution on Γ, we obtain a system of two coupled integral equations (Ingham & Kelmanson 1984):

$$\begin{aligned}\psi(s) = {} & \frac{1}{\pi}\int_\Gamma \psi(\tilde{s})\frac{\partial}{\partial n}\log|\boldsymbol{r}(\tilde{s})-\boldsymbol{r}(s)|\,\mathrm{d}\tilde{s} - \frac{1}{\pi}\int_\Gamma \psi'(\tilde{s})\log|\boldsymbol{r}(\tilde{s})-\boldsymbol{r}(s)|\,\mathrm{d}\tilde{s} \\ & + \frac{1}{4\pi}\int_\Gamma \omega(\tilde{s})\frac{\partial}{\partial n}\{\boldsymbol{r}(\tilde{s})-\boldsymbol{r}(s)\}^2\{\log|\boldsymbol{r}(\tilde{s})-\boldsymbol{r}(s)|-1\}\,\mathrm{d}\tilde{s} \\ & - \frac{1}{4\pi}\int_\Gamma \omega'(\tilde{s})\{\boldsymbol{r}(\tilde{s})-\boldsymbol{r}(s)\}^2\{\log|\boldsymbol{r}(\tilde{s})-\boldsymbol{r}(s)|-1\}\,\mathrm{d}\tilde{s}, \end{aligned} \tag{9}$$

$$\omega(s) = \frac{1}{\pi}\int_\Gamma \omega(\tilde{s})\frac{\partial}{\partial n}\log|\boldsymbol{r}(\tilde{s})-\boldsymbol{r}(s)|\,\mathrm{d}\tilde{s} - \frac{1}{\pi}\int_\Gamma \omega'(\tilde{s})\log|\boldsymbol{r}(\tilde{s})-\boldsymbol{r}(s)|\,\mathrm{d}\tilde{s}, \tag{10}$$

where $\boldsymbol{r}(s)$ and $\boldsymbol{r}(\tilde{s})$ denote position vectors on Γ. It is understood that the normal derivative $\partial/\partial n$ is taken with respect to the current vector $\boldsymbol{r}(\tilde{s})$, i.e. $\boldsymbol{r}(\tilde{s})$ is allowed to vary in an infinitesimal sense along a line normal to Γ. Therefore we have

$$\frac{\partial \boldsymbol{r}(\tilde{s})}{\partial n} = \boldsymbol{n}. \tag{11}$$

To illustrate this we derive (figure 2)

$$\frac{\partial}{\partial n}\log|\boldsymbol{r}(\tilde{s})-\boldsymbol{r}(s)|\,\mathrm{d}s = \boldsymbol{n}\cdot\frac{\boldsymbol{r}(\tilde{s})-\boldsymbol{r}(s)}{|\boldsymbol{r}(\tilde{s})-\boldsymbol{r}(s)|}\frac{\mathrm{d}s}{|\boldsymbol{r}(\tilde{s})-\boldsymbol{r}(s)|} = \frac{\mathrm{d}l}{|\boldsymbol{r}(\tilde{s})-\boldsymbol{r}(s)|} = \mathrm{d}\theta, \tag{12}$$

which is a well-known result. The integrand of the first integral appearing in (9) becomes singular and non-integrable when $\tilde{s} = s$. A finite value is obtained by defining the integral as the principal value, i.e by excluding $\tilde{s} = s$ from the integration path and approaching this point from both sides at the same rate.

We have solved the integral equations (9) and (10) together with the boundary conditions (5) and (6) numerically by replacing Γ by a polygon. The vertices of this polygon are given by $(x_i, y_i), i = 1, m$ in any Cartesian coordinate system (x, y). In each of these vertices, which we shall also use as collocation points, the functions $\psi(s)$, $\psi'(s)$, $\omega(s)$ and $\omega'(s)$ are given by the, as yet unknown, values $\psi_i, \psi_i', \omega_i, \omega_i'$ respectively. Each of the integrals appearing in (9) and (10) is now replaced by a sum

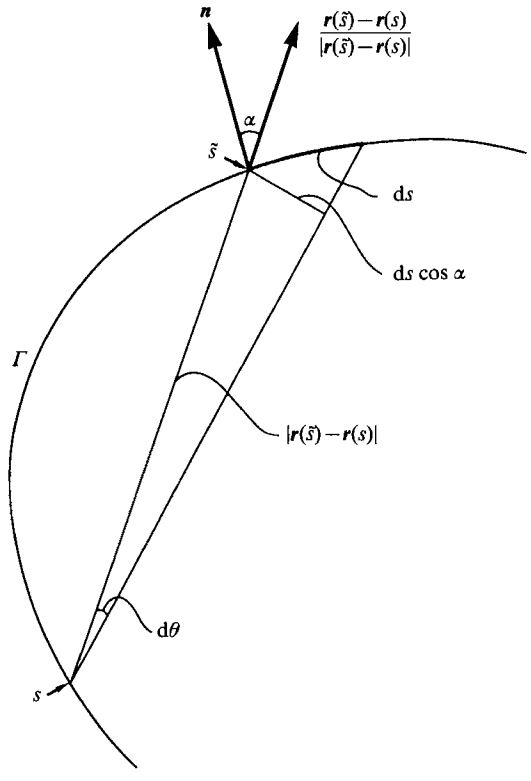

FIGURE 2. Graph explaining the derivation of (12).

of m integrals, one along each of the sides of the polygon. In between the vertices the unknown functions are obtained by linear interpolation. For instance

$$\psi(\tilde{s}) \approx \frac{1}{\delta_i}\{(s_{i+1}-\tilde{s})\,\psi_i+(\tilde{s}-s_i)\,\psi_{i+1}\}, \quad (s_i < \tilde{s} < s_{i+1}), \tag{13}$$

where

$$\delta_i = s_{i+1}-s_i. \tag{14}$$

Ingham & Kelmanson (1984) assume ψ and ω constant on each of the subintervals defined by (13). The present approach can be expected to yield more accurate results, but the algebra becomes rather more awkward.

When (13), and a similar equation for ω, are substituted in (9) and (10), two sets of linear equations involving ψ_i, ω_i and their derivatives with respect to s result:

$$\sum_{j=1}^{m} A_{ij}\psi_j+B_{ij}\psi_j'+C_{ij}\omega_j+D_{ij}\omega_j' = 0 \quad (i = 1,2,\ldots,m), \tag{15}$$

$$\sum_{j=1}^{m} A_{ij}\omega_j+B_{ij}\omega_j' = 0 \quad (i = 1,2,\ldots,m). \tag{16}$$

The coefficients A_{ij}, B_{ij}, C_{ij} and D_{ij} involve complicated integrals over each of the subintervals defined by (14). These integrals can be evaluated analytically (Kuiken 1990), which reduces the numerical work substantially.

In addition to the $2m$ equations (15) and (16) there is another set of $2m$ equations

resulting from the two boundary conditions (5) and (6). The character of these boundary conditions is that of two coupled second-order ordinary differential equations. These can be discretized in an obvious manner. This and other particulars of the numerical method are explained in the aforementioned companion paper (Kuiken 1990) to which we refer the interested reader. The end result of the discretization process is a set of $4m \times 4m$ linear equations for the unknowns ψ_i, ψ_i', ω_i and ω_i' defined in the collocation points. The first set of $2m$ equations results from the integral equations (9) and (10). The remaining $2m$ are the discretized analogues of the two boundary conditions (5) and (6). The parts of the matrix which result from these last contributions are sparse. This enables us to reduce the $4m \times 4m$ matrix to one that is only $2m \times 2m$, which helps a great deal in limiting the computer time needed to solve the title problem.

We can now simulate the motion of the boundary Γ by a time-stepping process which results when we apply a simple forward Euler rule to the moving-boundary condition (7), subject to the initial condition (8). Higher-order approaches to this aspect of the problem are possible, but it would not seem reasonable to explore the merits of these before the stability problem we shall discuss later has been dealt with successfully.

4. The damping of small disturbances

It will be of interest to know how small disturbances are damped by a system which flows solely under the influence of tangential gradients in the curvature of its outer boundary. If the disturbances are small in relation to the size of the system itself, we are justified in considering the fluid system to be infinitely large. We shall therefore use a Cartesian coordinate system (x, y) in which to describe it, assuming that the equilibrium outer surface coincides with $y = 0$. The disturbed surface, which is not in equilibrium, is at $y = f(x)$, the fluid residing in $y \leqslant f(x)$, $-\infty < x < \infty$. Since the disturbance is small, we have $|f| \ll 1$ and $|\mathrm{d}f/\mathrm{d}x| \ll 1$ for all x. All the dependent variables, viz. ψ and ω, are small as well. Therefore, in the spirit of an ordinary perturbation approach, we can take the boundary conditions (5) and (6) on $y = 0$, neglecting the nonlinear terms, i.e.

$$\omega = 2\frac{\partial^2\psi}{\partial x^2}, \quad 2\frac{\partial^3\psi}{\partial x^2\,\partial y}+\frac{\partial\omega}{\partial y} = -\frac{\mathrm{d}^3 f}{\mathrm{d}x^3} \quad \text{on} \quad y = 0 \quad (-\infty < x < \infty). \tag{17a, b}$$

The field equations are given by (3) and (4). In the derivation of (17*b*) we approximated κ by $\mathrm{d}^2 f/\mathrm{d}x^2$, which is the leading term in a small-term expansion of the curvature.

The linear boundary-value problem defined above can be solved by means of the Fourier transform. The solution for ψ is found to be

$$\psi = \frac{\mathrm{i}}{4\pi}\int_{-\infty}^{\infty}\left(\frac{\mu}{|\mu|}-\mu y\right)\bar{f}(\mu)\,\mathrm{e}^{|\mu|y-\mathrm{i}\mu x}\,\mathrm{d}\mu, \tag{18}$$

where it should be remembered that $y \leqslant 0$ everywhere in the flow field. In (18) $\bar{f}(\mu)$ is the Fourier transform of f, viz.

$$\bar{f}(\mu) = \int_{-\infty}^{\infty}\mathrm{e}^{\mathrm{i}\mu x} f(x)\,\mathrm{d}x. \tag{19}$$

The vertical velocity of the boundary can now easily be derived:

$$v = -\frac{\partial \psi}{\partial x}\bigg|_{y=0} = -\frac{\mathrm{i}}{4\pi}\frac{\mathrm{d}}{\mathrm{d}x}\int_{-\infty}^{\infty}\frac{\mu}{|\mu|}\bar{f}(\mu)\,\mathrm{e}^{-\mathrm{i}\mu x}\,\mathrm{d}\mu. \tag{20}$$

Using (19) we have

$$\begin{aligned}\frac{\mathrm{i}}{2}\int_{-\infty}^{\infty}\frac{\mu}{|\mu|}\bar{f}(\mu)\,\mathrm{e}^{-\mathrm{i}\mu x}\,\mathrm{d}\mu &= \int_{-\infty}^{\infty} f(p)\,\mathrm{d}p\int_{0}^{\infty}\sin\mu(x-p)\,\mathrm{d}\mu \\ &= \lim_{\lambda\to\infty}\int_{-\infty}^{\infty} f(p)\,\mathrm{d}p\int_{0}^{\lambda}\sin\mu(x-p)\,\mathrm{d}\mu \\ &= \lim_{\lambda\to\infty}\int_{0}^{\infty}\frac{f(x-q)-f(x+q)}{q}\{1-\cos\lambda q\}\,\mathrm{d}q \\ &= \int_{0}^{\infty}\frac{f(x-q)-f(x+q)}{q}\,\mathrm{d}q, \end{aligned} \tag{21}$$

so that

$$v = \frac{1}{2\pi}\int_{0}^{\infty}\left\{\frac{\mathrm{d}f}{\mathrm{d}x}(x+q)-\frac{\mathrm{d}f}{\mathrm{d}x}(x-q)\right\}\frac{\mathrm{d}q}{q}, \tag{22}$$

where a prime stands for differentiation with respect to the argument.

If we now consider the boundary as a function of both x and τ, where τ is the dimensionless time, then we have

$$v = \frac{\partial f}{\partial \tau} \tag{23}$$

and, using (22), we can deduce an integro-differential equation for $f(x,\tau)$:

$$\frac{\partial f}{\partial \tau} = \frac{1}{2\pi}\int_{0}^{\infty}\left\{\frac{\partial f}{\partial x}(x+q,\tau)-\frac{\partial f}{\partial x}(x-q,\tau)\right\}\frac{\mathrm{d}q}{q}, \tag{24}$$

which is subject to the initial condition

$$f(x,0) = f_0(x) \tag{25}$$

and conditions at infinity:

$$f\to 0 \quad \text{when} \quad |x|\to\infty \quad (\text{all } \tau \geqslant 0). \tag{26}$$

With aid of both the Laplace and the Fourier transforms we are able to derive the solution of (24) which satisfies (25) as follows:

$$f(x,\tau) = \frac{\tau}{2\pi}\int_{-\infty}^{\infty} f_0(x-p)\frac{\mathrm{d}p}{\frac{1}{4}\tau^2+p^2}. \tag{27}$$

As an example we consider

$$f_0(x) = \frac{1}{1+x^2}. \tag{28}$$

In considering (28) we should realize that the shape of the original surface is $\epsilon f_0(x)$, but that we have scaled out the small parameter ϵ in conformity with our perturbation approach. Substituting (28) in (27) we find after some manipulation

$$f(x,\tau) = \frac{1+\frac{1}{2}\tau}{x^2+(1+\frac{1}{2}\tau)^2} \tag{29}$$

and
$$v = \frac{1}{2}\frac{x^2-(1+\frac{1}{2}\tau)^2}{\{x^2+(1+\frac{1}{2}\tau)^2\}^2}. \tag{30}$$

It is interesting to see that for $|x| > 1$ the boundary moves upwards first before it moves downwards permanently. At any time τ the boundary is still moving upwards when $|x| > 1+\frac{1}{2}\tau$. Only the part of the boundary for which $|x| < 1$ moves in a downward direction right from the start.

Another matter worth looking into is how fast wriggles in the surface are evened out. Let us consider
$$f_0(x) = \cos \omega x, \tag{31}$$

where again we have scaled out the small parameter ϵ which determines the actual elevation of the surface above $y = 0$. Substituting (31) in (27) we find
$$f(x,\tau) = \mathrm{e}^{-\frac{1}{2}\tau\omega} \cos \omega x. \tag{32}$$

Clearly, a larger frequency ω leads to a faster damping process. We should realize that we cannot let ω grow indefinitely, since the analysis becomes invalid for those larger ω-values. Indeed, in the approximation of the curvature leading to (17) we disregarded $\mathrm{d}f_0/\mathrm{d}x$ in comparison with unity. We are only permitted to do so as long as $\epsilon\omega \ll 1$.

There is a striking difference between the asymptotic properties of (29) and (32) for $\tau \to \infty$. Apparently, a non-oscillating boundary form is flattened out at a much slower pace than one which oscillates throughout. Assuming that $f_0(x)$ tends to zero fast enough for $|x| \to \infty$, we obtain from (27)
$$f(0,\tau) \sim \frac{2}{\pi\tau}\int_{-\infty}^{\infty} f_0(p)\,\mathrm{d}p \quad \text{for} \quad \tau \to \infty. \tag{33}$$

Therefore, if the integral appearing in (33) differs from zero, the damping velocity is eventually inversely proportional to time. Faster damping velocities are achieved if the integral is equal to zero. This condition means that the average elevation of the disturbed surface above the plane $y = 0$ is equal to zero, which seems physically quite realistic.

5. Results and discussion

A computer program has been written on the basis of the model presented in this paper. To give an idea of the kind of results that can be obtained with it, we present figures 3(*a*) and 4(*a*). The first of these shows how the ellipse $x^2+10y^2 = 1$ is transformed into a circle, the second in what way a dent disappears. As expected, order-one changes in shape are achieved when the dimensionless time τ reaches values that are of order unity. In fact, the final shapes in figures 3(*a*) and 4(*a*), which appear to be circular to the eye, were obtained for $\tau = 10$.

Figures 3(*b*) and 4(*b*) reveal how particles on the surface move in time. Contrary to what figure 4(*a*) would seem to suggest, figure 4(*b*) shows that all material points on the surface move a considerable distance during the process of deformation. This is also true for the points in the region where consecutive shapes intersect. Figure 4(*b*) demonstrates that certain material points traverse fairly curved paths on their way from the initial shape to the final one.

The examples of figures 3 and 4 refer to shapes for which the curvature function $\kappa(s)$ varies only moderately. It would be of further interest, particularly with a view to real sintering situations such as the confluence of two spheres, if we could tackle

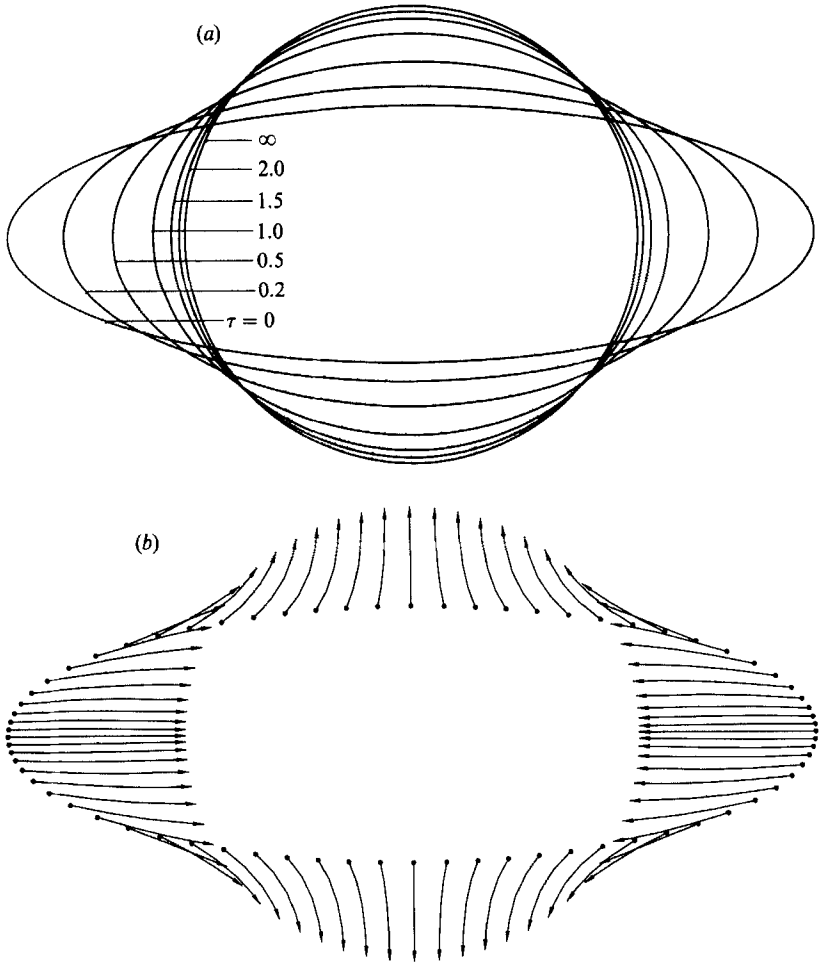

FIGURE 3. (a) The transformation of an ellipse into a circle. The various graphs refer to shapes for various values of the time τ. (b) The paths followed by material points of the boundary. The deformation process is that of figure 4 (a). The arrows denote both the direction of flow and the final positions of the material points. The dots refer to the initial positions.

initial shapes such as that of figure 1. Unfortunately, in its present form, our numerical procedure seems to be unable to handle these more extreme forms. The reason is to be found in the fact that a discretized representation of Γ leads to inaccuracies in $\mathrm{d}\kappa/\mathrm{d}s$ which, as one can see from (6), is the driving force in the problem at hand. Clearly, round-off errors are always present, and these affect the position vector $\boldsymbol{r}(s,\tau)$ directly. Inaccuracies of the position vectors lead to much increased inaccuracies in the curvature function $\kappa(s)$. Since the driving force is obtained by a further differentiation, the resulting inaccuracies may seriously affect the time-stepping process.

Of course, a periodic smoothing of the data defining Γ may be a remedy for these ills. However, numerical smoothing is somehow an added physical phenomenon in disguise, a phenomenon which was not part of the original continuous model. If the effect associated with this phenomenon is stronger than the driving force relating to the curvature gradients, then adding this particular smoothing procedure means that we are solving some problem, but not the one we intended to solve at the outset.

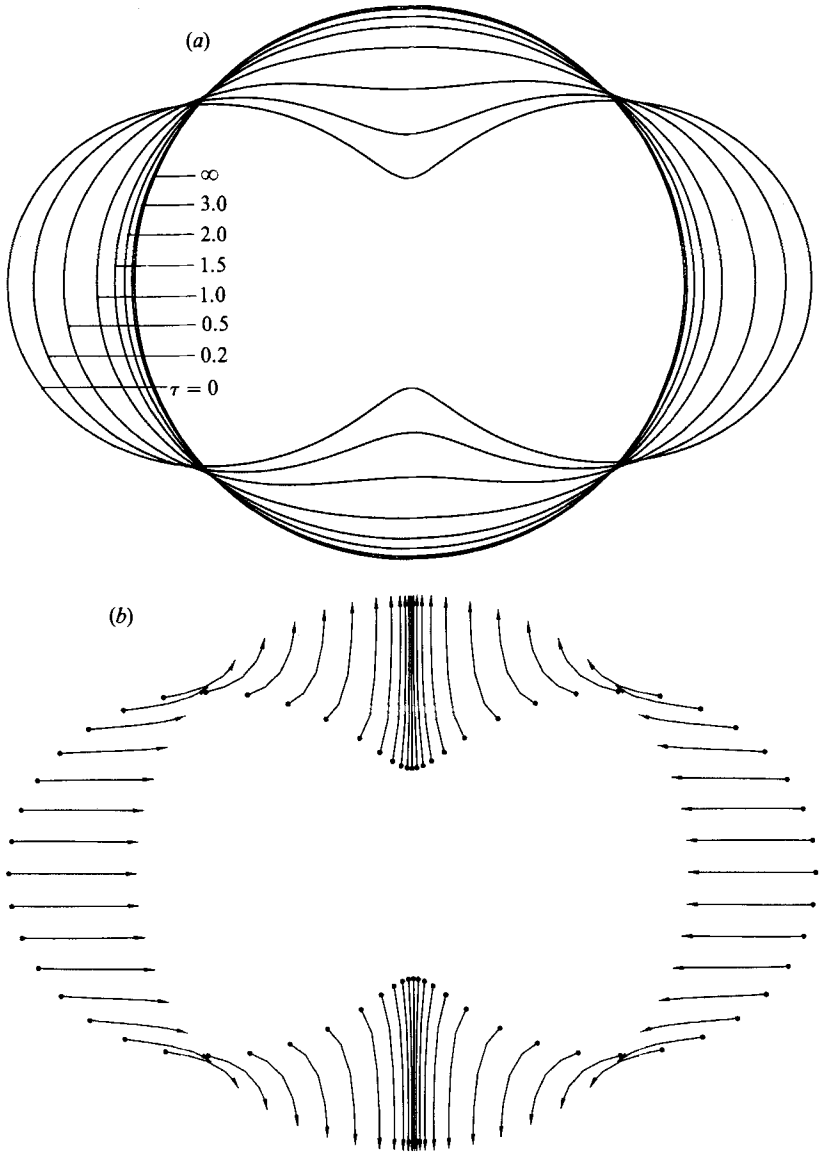

FIGURE 4. (*a*) The deformation of another liquid form. (*b*) Motion of material boundary points of the shape depicted by figure 4(*a*).

As we have seen, rapid oscillations of Γ are damped rapidly by the continuous model. Our analytical treatment of small disturbances gave ample proof of this. However, when sampling a boundary fraught with rapid small-amplitude oscillations, as we are doing when we represent Γ by a polygon, the values of $\kappa(s)$, and most certainly those of $\mathrm{d}\kappa/\mathrm{d}s$, that we get are no longer representative of the average values of $\kappa(s)$ and $\mathrm{d}\kappa/\mathrm{d}s$. But these average values, on the whole, determine the average deformation behaviour of Γ. See for instance figure 5, where we have represented the curve $x^2+10y^2 = 1$ along with a rapid oscillation of small amplitude superposed upon it. Our small-disturbance analysis shows that the oscillatory behaviour will disappear exponentially fast, and the subsequent flow behaviour will

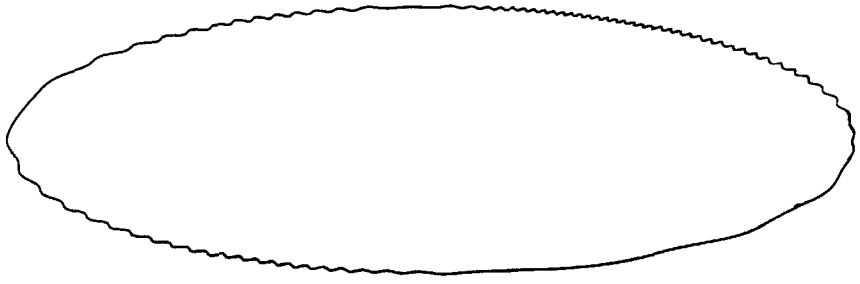

FIGURE 5. A shape spoiled by rapid oscillations of a kind that may be generated by the numerical process.

be that depicted in figure 3(*a*). The present numerical process, on the other hand, will fail to simulate this natural process, since a sampling of the curve of figure 5 will lead to a wildly varying driving force. Clearly, some kind of smoothing will have to be carried out here. The question is: how to define an honest smoothing routine which does not represent a dominant physical effect that relegates the real driving force to only a second position?

It was pointed out to the author by S. Richardson (1989, personal communication) that, strictly speaking, the model given by (3)–(6) does not ensure a unique solution. Indeed, a superimposition of an arbitrary rigid-body translation and an arbitrary rigid-body rotation upon any particular solution will not alter the stress field at the outer boundary. Richardson suggests that in addition to (5) and (6) we should require that both linear and angular momentum vanish. In our two numerical examples these two conditions are satisfied automatically, on account of the double symmetry.

The older theories of sintering, e.g. Frenkel (1945) or Scherer (1977), exploit the global rule which states that the total work done by surface tension to reduce the outer surface area should be equal to the heat released by viscous dissipation. It may be worthwhile to illustrate this rule here. In normalized terms the rate at which work is done by surface tension is given by

$$W_{\text{surf}} = -\frac{\mathrm{d}}{\mathrm{d}\tau}\int_{\Gamma(\tau)} \mathrm{d}s, \tag{34}$$

where, as before, τ is the time, $\Gamma(\tau)$ is the closed curve which encloses the viscous region Ω, and s is the arclength. Using some well-known rules, we may rewrite (34) as follows:

$$W_{\text{surf}} = -\int_{\Gamma} \boldsymbol{t}\cdot\frac{\mathrm{d}\boldsymbol{u}}{\mathrm{d}s}\mathrm{d}s = \int_{\Gamma} \boldsymbol{u}\cdot\frac{\mathrm{d}\boldsymbol{t}}{\mathrm{d}s}\mathrm{d}s = \int_{\Gamma} \kappa\boldsymbol{u}\cdot\boldsymbol{n}\,\mathrm{d}s, \tag{35}$$

where $\boldsymbol{u}$ is the velocity vector, $\boldsymbol{t}$ the tangent vector along Γ and $\boldsymbol{n}$ the outward normal which is obtained from $\boldsymbol{t}$ by an anticlockwise rotation.

To obtain an expression for the heat of dissipation we refer to Batchelor (1967, pp. 152–153). In Batchelor's notation we have

$$W_{\text{diss}} = \int_{\Omega} \frac{\partial}{\partial x_j} u_i \sigma_{ij}\,\mathrm{d}A = \int_{\Gamma} u_i \sigma_{ij} n_j\,\mathrm{d}s, \tag{36}$$

where σ_{ij} is the stress tensor and u_i represents the components of the velocity vector $\boldsymbol{u}$ in some Cartesian coordinate system x_i. Since $\sigma_{ij} n_j$ is the force acting on the boundary Γ, we have

$$\sigma_{ij} n_j = \kappa n_i, \tag{37}$$

from which we have $$W_{\text{diss}} = W_{\text{surf}}. \tag{38}$$

Finally, we remark that the relevance of the method developed here for the simulation of sintering processes is limited to the later stages of these processes, when the curvature of the internal surface of the compact shows only moderate variations. As a possible application we may think of the classic problem first studied by Mackenzie & Shuttleworth (1949). Considering a unit cell of a compact consisting of a regular array of spherical bubbles of equal size embedded in a viscous liquid, we have a problem that we might be able to solve with the present method. Of course, as it now stands, our method can be applied only to a two-dimensional analogue of this problem.

Note added in proof. While the present paper was in the hands of the referees, the author discovered that Dr R. W. Hopper of Lawrence Livermore National Laboratory (California, USA) had succeeded in getting analytical solutions for certain classes of two-dimensional viscous-sintering problems. Among these is the important two-cylinder problem. (See Hopper 1990*a*, *b*, *c*.)

REFERENCES

Batchelor, G. K. 1967 *An Introduction to Fluid Dynamics*. Cambridge University Press.

Exner, H. E. 1979 *Rev. Powder Metall. Phys. Ceram.* **1**, 7–251.

Frenkel, J. 1945 *J. Phys. USSR* **9**, 385–391.

Fricke, J. 1988 *Sci. Am.* **258** (May), 68–73.

Geguzin, Ja. E. 1973 *Physik des Sinterns*. Leipzig: VEB Deutscher verlag Grundstoffindustrie.

Hopper, R. W. 1990 Plane Stokes flow driven by capillarity on a free surface. *J. Fluid Mech.* **213**, 349–375.

Hopper, R. W. 1990*b* Plane Stokes flow driven by capillarity, Part 2. Coalescence of unequal cylinders. *J. Fluid Mech.* (submitted).

Hopper, R. W. 1990*c* Plane Stokes flow driven by capillarity, Part 3. Unbounded regions. *J. Fluid Mech.* (submitted).

Ingham, D. B. & Kelmanson, M. A. 1984 *Boundary Integral Equation Analyses of Singular, Potential and Biharmonic Problems*. Lecture Notes in Engineering, vol. 7. Springer.

Kuczinsky, G. C. 1949*a* *Metall. Trans. AIME* **185**, 169–178.

Kuczinsky, G. C. 1949*b* *J. Appl. Phys.* **20**, 1160–1163.

Kuiken, H. K. 1990 *Proc. Conf. on the Mathematics and the Computation of Deforming Surfaces*. Oxford University Press (to appear).

Mackenzie, J. K. & Shuttleworth, R. 1949 *Proc. Phys. Soc. Lond.* **62**, 833–852.

Reed, J. S. 1988 *Introduction to the Principles of Ceramic Processing*. John Wiley & Sons.

Scherer, G. W. 1977 *J. Am. Ceram. Soc.* **60**, 236–239.

Scherer, G. W. 1984 *J. Am. Ceram. Soc.* **67**, 709–715.